Development of electron holes across the temperature-induced semiconductor–metal transition in $Ba_{1-x}Sr_xCo_{1-y}Fe_yO_{3-\delta}$ (x, y = 0.2–0.8): a soft x-ray absorption spectroscopy study

2009 J. Phys.: Condens. Matter 21 015801

(http://iopscience.iop.org/0953-8984/21/1/015801)

J. Phys.: Condens. Matter **21** (2009) 015801 (10pp) doi:10.1088/0953-8984/21/1/015801

Development of electron holes across the temperature-induced semiconductor–metal transition in $Ba_{1-x}Sr_xCo_{1-y}Fe_yO_{3-\delta}$ (x, $y = 0.2$–0.8): a soft x-ray absorption spectroscopy study

A S Harvey[1,3], Z Yang[1], A Infortuna[1], D Beckel[1], J A Purton[2] and L J Gauckler[1]

[1] Nonmetallic Inorganic Materials, Department of Materials, ETH Zurich, Wolfgang-Pauli-Strasse 10, CH-8093 Zurich, Switzerland
[2] Science and Technology Facilities Council, Daresbury Laboratory, Warrington WA4 4AD, UK

E-mail: ashley.harvey@mat.ethz.ch

Received 16 June 2008, in final form 7 October 2008
Published 2 December 2008
Online at stacks.iop.org/JPhysCM/21/015801

Abstract

The x-ray absorption spectra of $Ba_{1-x}Sr_xCo_{1-y}Fe_yO_{3-\delta}$ (BSCF) powders quenched in air from 623 and 1173 K were measured at the oxygen K and transition metal $L_{II,III}$ edges. All the samples show a predominantly Fe high spin ground state of $3d^5\underline{L}$ character, while the $3d^6\underline{L}$ Co ions are intermediate spin at 623 K and high spin at 1173 K. Further changes in the metal $L_{II,III}$ peaks caused by higher temperature quenching are attributed to changes in symmetry around the cations associated with oxygen loss. The oxygen K spectra show the development of unoccupied states just above the Fermi level for samples quenched from 1173 K. At 1173 K, $Ba_{1-x}Sr_xCo_{1-y}Fe_yO_{3-\delta}$ shows metallic conductivity, while at 623 K it is a semiconductor; the states developed at high temperature with strong oxygen character are pathways for hole conductivity. Splitting of the transition metal 3d energy levels by the ligand field was observed in the oxygen K spectra, and the range for $10Dq$ is 1.6–1.8 eV, while the 3d bandwidth is 1.1–1.4 eV in samples quenched from 623 K. On the basis of the soft x-ray absorption results, the classification of $Ba_{1-x}Sr_xCo_{1-y}Fe_yO_{3-\delta}$ as a material with a negative charge-transfer energy is proposed.

1. Introduction

Perovskite oxides, of the general chemical formula ABO_3, have been a rich area of study for their inherent ability to accept many different elements on the A and B lattice sites and resultant physical properties. Examples of the extraordinary characteristics of perovskites include superconductivity [1], colossal magnetoresistance [2], and metal–insulator transitions driven by composition or temperature changes [3, 4]. The oxygen stoichiometry can also be altered and as such, many perovskites exhibit oxygen ion conductivity via oxygen vacancies. Perovskite materials involving Co and Fe are particularly interesting as they lie near the boundary between lower-Z transition metal oxides with Mott–Hubbard electronic behavior and higher-Z transition metal oxides with charge-transfer behavior; some compositions with high transition metal oxidation states are negative charge-transfer materials [5–8].

The band structure as related to such compounds has been rationalized in terms of the interplay of the Coulomb interaction U with the charge-transfer energy Δ_{ct}, transfer integral T, and bandwidth W as described in the well-known

[3] Author to whom any correspondence should be addressed.

work of Zaanen *et al* [9]. The crystal field splitting of the B-site transition metal 3d levels by the surrounding oxygen ions with octahedral coordination results in the triply degenerate t_{2g} and doubly degenerate e_g levels separated by $10Dq$. Transition metals with six 3d electrons exhibit competition between Hund's energy, which promotes spin alignment, and the crystal field splitting, which can stabilize lower spin states. If the exchange energy Δ_{ex} is less than $10Dq$, the low spin ground state will dominate. In the perovskites, conductivity occurs along the B–O–B chains through the electron/hole transfer between the transition metal t_{2g} and O 2p orbitals. The Coulomb potential Ze^2/r of both the A- and B-site cations influences the spatial extent of the t_{2g} orbitals: increasing the potential at either site decreases overlap, while increasing the attraction between the B and O ions increases the overlap, creating wider bands [10]. A randomized mixed occupancy of the B site is expected to disrupt the potential across the B–O–B bonds and prevent metallic conductivity, but B-site ordering could restore the periodicity.

$Ba_{1-x}Sr_xCo_{1-y}Fe_yO_{3-\delta}$ (BSCF) exhibits structural stability even with large oxygen non-stoichiometry ($\delta \geqslant 0.5$) [11] and has high oxygen permeability [12]. A main advantage of BSCF over similar materials is that it exhibits a mixed electronic–ionic conductivity. Measurements of the total conductivity show a transition from semiconducting to metallic in the range of 670–820 K, depending on the composition [13, 14]. Similar to other perovskites, the temperature-dependent conductivity mechanism is thought to be p-type small polaron hopping along with super-exchange in antiferromagnetic materials [14, 15] and double-exchange in ferromagnetic materials [16]. Recently BSCF with $x = 0.5$, $y = 0.2$ was identified as a good cathode for solid oxide fuel cells [17], though the longevity of the material under typical operating conditions is still not clear [18].

While the end members of the BSCF system ($x, y = 0, 1$) are difficult to synthesize in the cubic perovskite structure and are typically oxygen deficient unless prepared in high oxygen pressure [19, 20], doping at either the A or B site stabilizes the structure [21]. Over most values of x and y, the undistorted cubic structure with space group $Pm\bar{3}m$ is formed, but for $x \leqslant 0.2$ and $y < 0.2$ distortions and vacancy ordering occur [13, 22, 23]. Heating BSCF in air results in the continuous loss of oxygen at a temperature onset around 673 K [13] and with fixed concentrations of divalent cations at the A site, this process should be accompanied by reduction of the B-site ions, as in β oxygen desorption [24]. Little work on the magnetic properties of BSCF has been done, but for the composition with $x = 0.8$, $y = 0.2$, a ferrimagnetic transition was found at 700 K [25], and through refinement of neutron diffraction patterns, the composition with $x = 0.5$, $y = 0.2$ showed a G-type antiferromagnetic structure at room temperature with 2.48(1) μ_B per B-site ion [11].

Previous x-ray absorption spectroscopy work by Abbate *et al* demonstrated that even perovskites with B-site atoms different only by $Z = 1$ ($LaMnO_3$ and $LaFeO_3$) exhibit different reactions to the creation of holes by Sr^{2+} doping [26]. With BSCF, it is not only interesting to study the subtle changes induced by the relatively minor changes in composition, but also the nature of the conduction behavior. In this paper, we aim to identify the oxidation states of Fe and Co in BSCF samples quenched from the semiconducting (medium temperature) and metallic (high temperature) states, under the assumption that rapid cooling preserves the characteristics of the heated material. Furthermore, we investigate the interaction of the transition metal 3d electrons with the oxygen 2p and the character of the holes as part of the mechanism of metallic conductivity. For these purposes, x-ray absorption spectroscopy measurements were carried out at the transition metal $L_{II,III}$ and oxygen K edges.

2. Methods

$Ba_{1-x}Sr_xCo_{0.8}Fe_{0.2}O_{3-\delta}$ ($x = 0.2, 0.4, 0.5, 0.6, 0.8$) and $Ba_{0.5}Sr_{0.5}Co_{1-y}Fe_yO_{3-\delta}$ ($y = 0.2, 0.4, 0.6, 0.8$) powders were synthesized via solid state reaction and subsequently calcined to achieve perovskite structures as the primary phase. The details of the processing will be published elsewhere [23]. For the quenching experiment, approximately 5 g of each powder was pressed into disks 1 cm in diameter. Two disks of each composition were made, with one of each heated to 623 K and the other to 1173 K in air. The samples were held at these elevated temperatures for 24 h and withdrawn from the furnace to quench to room temperature on the bench top.

X-ray absorption spectroscopy (XAS) is a method based on the x-ray induced promotion of electrons from core energy levels to unoccupied states. This phenomenon can be recorded in a variety of ways: (1) for transmission, if the x-ray energy is high enough, the attenuation of the beam can be directly measured; (2) with fluorescence yield, the emission of x-rays resulting from the de-excitation of the atoms is measured; and (3) in total electron yield, the Auger, photoemission, scattered, and secondary electrons resulting from the de-excitation are collected. Only the latter two are used for absorption edges < 2000 eV, encompassing the O K and Fe/Co $L_{II,III}$ edges. With each method comes a different probing depth, and electron yield has the smallest, at about 5 nm. Further, there is competition between the fluorescence and Auger processes, with the fluorescence yield for elements with $Z < 30$ being much less than the electron yield. Because of the simplicity of the technique and its prevalence in the literature cited herein, total electron yield was the XAS detection method chosen for the present experiments.

For the XAS measurements, some of each sample was finely ground and spread on a piece of carbon sticky tape affixed to the sample holder immediately before putting the sample holder into the vacuum chamber to minimize contamination. The chamber had a pressure of about 10^{-7} mbar. The XAS data were gathered in total electron yield (TEY) at beamline 1.1 of the Daresbury Laboratory Synchrotron Radiation Source (SRS), which is equipped with a high energy spherical grating monochromator [27]. Spectra of the oxygen K and transition metal $L_{II,III}$ edges were gathered with energy resolutions of 0.25 eV at 530 eV and 0.45 eV at 780 eV with a 0.1 mm exit slit. These resolution values are similar to the intrinsic core–hole lifetime broadening of the $L_{II,III}$ edges [28]. The primary beam intensity (I_0) was

measured by the total current from a gold grid placed in the x-ray path before the sample chamber. The ring energy was 2.0 GeV with current ranging from about 150 to 200 mA.

Data processing of the XAS spectra (I/I_0 as a function of x-ray energy) was performed using the Athena program of the Ifeffit software suite [29]. Spectra were aligned to constant features in the I_0 signal, background-subtracted, and normalized to the area of the spectrum 10–40 eV above the edge onset for the Fe and Co $L_{II,III}$ spectra and 30–100 eV above the edge for the O K.

X-ray diffraction (XRD) patterns were obtained from the crushed powders of the quenched samples using a Siemens D5000 Diffractometer with Cu Kα radiation. The patterns were analyzed for crystal structure and lattice parameters with the software program X'Pert Highscore Plus (PANalytical, Spectris).

3. Results and interpretation

3.1. XRD

$Ba_{1-x}Sr_xCo_{1-y}Fe_yO_{3-\delta}$ samples that originated as $Pm\bar{3}m$ cubic perovskites ($x = 0.4$–0.8, $y = 0.4$–0.8, space group #221) from the calcining procedure remained so after quenching. Most samples showed slight impurities (up to about 2% mass) after calcining that remained with the heat treatment at 623 K, but all became pure cubic perovskites after quenching from 1173 K. One sample, $x = y = 0.2$, had two phases after calcination and quenching from 623 K, primarily the cubic perovskite and secondarily a related hexagonal structure. Quenching from the higher temperature resulted in expanded unit cell volumes in comparison to slowly cooled samples. XRD with *in situ* heating also shows a regularly increasing lattice parameter with increasing temperature for cubic BSCF samples [30]. Of course, the volume expansion of the quenched samples is not as great as that observed *in situ*: it is about 1/4 the magnitude. Since the XRD patterns of the quenched samples were measured at room temperature, we can assume that the expansion of the cell volume in these materials is not due to thermal expansion, but results from chemical expansion concomitant with oxygen loss and changes in the electronic states of the cations. This is in agreement with neutron diffraction experiments, where it was observed that the lattice parameter of BSCF with $x = 0.5$ and $y = 0.2$ increased with increasing oxygen deficiency [11].

In general, increasing the amount of Ba and Co in the BSCF compositions increased the unit cell. The observed effect of Co concentration is informative, as when Fe and Co are of the same oxidation and spin states, the Fe ion is typically larger. Increasing the oxidation state decreases the ionic radius, while going from low to high spin or increasing the cation coordination does the opposite [31]. Assuming that the oxygen non-stoichiometry is not affected by different values of x and y (as long as $x, y \neq 0, 1$) and considering the cases of BSCF with cubic crystal structure, the increase in lattice parameter with increasing Co content could indicate that Co has a lower oxidation or spin state, and larger ionic radius, than Fe.

Table 1. Fe and Co branching ratios (BR) of $Ba_{1-x}Sr_xCo_{1-y}Fe_yO_{3-\delta}$ quenched from 623 and 1173 K (see figures 2 and 3). Branching ratios for (La, Sr)(Co, Fe)$O_{3-\delta}$ perovskites are given for comparison.

		Fe BR		Co BR	
x	y	623 K	1173 K	623 K	1173 K
0.8	0.2	0.80	0.79	0.71	0.77
0.5	0.2	0.81	0.81	0.69	0.79
0.2	0.2	0.81	0.81	0.69	0.79
0.5	0.8	0.81	0.79	0.70	0.77
$LaFeO_3$		0.81			
$SrFeO_{3-\delta}$		0.80			
$LaCoO_3$				0.69	
$SrCoO_{3-\delta}$				0.63	

3.2. Fe and Co $L_{II,III}$ XAS

The transition metal $L_{II,III}$ spectra result from electronic transitions from initial configurations of $2p^m d^n$ to final configurations of $2p^{m-1}d^{n+1}$ governed by the dipole and spin selection rules $\Delta L = \pm 1$, $\Delta S = 0$. The two multiplet structures—L_{II} at the higher energy side and L_{III} at the lower—arise from the spin–orbit interaction of the core hole with the valence electrons. In considering the origin of the changes in the metal $L_{II,III}$ spectra, we note that Fe and Co are in their respective high spin states when quenched from 1173 K. Quenching from 623 K may produce an intermediate spin state in the Co ions as has been discussed for similar materials $LaCoO_3$ and $SrCoO_3$, albeit at lower temperatures [8, 32].

For comparison, the Fe and Co $L_{II,III}$ spectra of $LaFeO_3$, $SrFeO_{3-\delta}$, $LaCoO_3$, and $SrCoO_{3-\delta}$ are shown in figure 1, and they match what has been previously found for these materials [8, 26, 32, 33]. The BSCF Fe $L_{II,III}$ spectra are shown in figure 2, with the set of data presented in figure 2(a) showing the effect of varying the Ba/Sr ratio and quenching temperature, while figure 2(b) shows the effect of varying Co/Fe and temperature. The spectra are normalized to the L_{II} peak areas and background. Branching ratios $I_{L_{III}}/(I_{L_{III}} + I_{L_{II}})$ for a selection of samples are given in table 1.

Changes in the Fe $L_{II,III}$ spectral shapes are not apparent when changing the composition at the quenching temperature of 623 K. For samples quenched from 1173 K, when varying the composition the peak ratio decreases with increasing iron and strontium. In comparing samples of the same composition quenched from different temperatures, the peak shapes are very similar, but those quenched from 1173 K have a smaller peak ratio than those from 623 K starting with $x, y \geqslant 0.4$ and decreasing to $x, y = 0.8$. In the two series $Ba_{1-x}Sr_xCo_{0.8}Fe_{0.2}O_{3-\delta}$ and $Ba_{0.5}Sr_{0.5}Co_{1-y}Fe_yO_{3-\delta}$, the spectra of the samples with the most Sr and Fe show the greatest changes with temperature. The peak shapes and branching ratios are most similar to samples with majority Fe^{3+} ions [26, 34] as compared to the spectra shown in figure 1, but the presence of ligand holes ($3d^5\underline{L}$) is very likely: the Fe spectra of BSCF appear as a mixture of those from $LaFeO_3$ and $SrFeO_{3-\delta}$ [5, 35]. That the iron is mainly $3d^5$ is not surprising as this has been found with similar materials [6, 36, 37].

The Co $L_{II,III}$ spectra are shown in figure 3, with the effect of varying the Ba/Sr ratio and quenching temperature shown

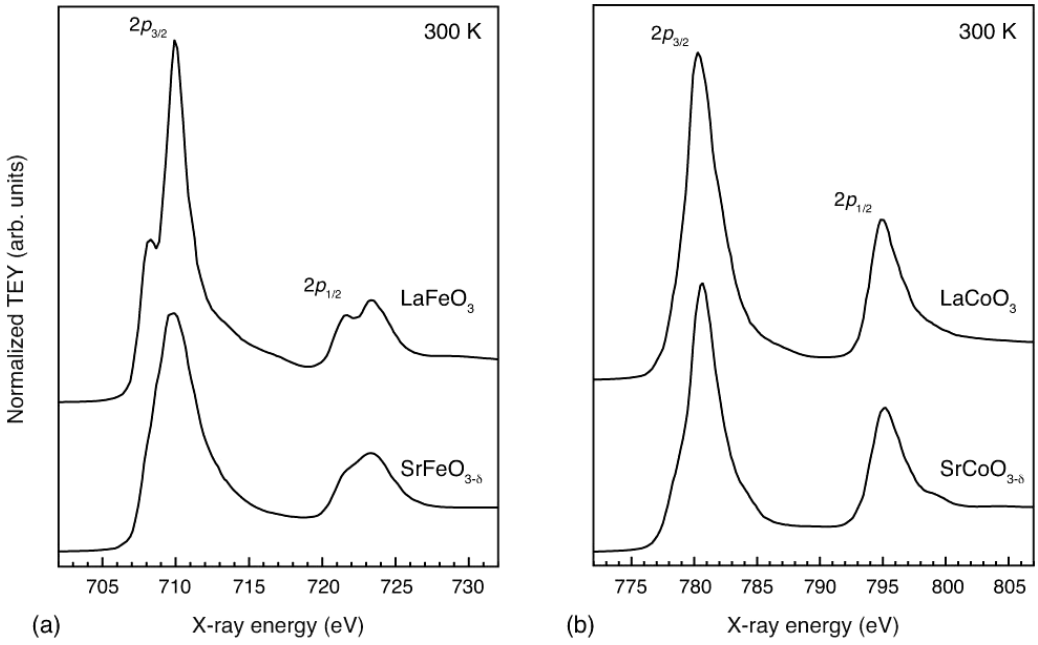

Figure 1. XAS of (a) Fe $L_{II,III}$ for $LaFeO_3$ and $SrFeO_{3-\delta}$ powders and (b) Co $L_{II,III}$ for $LaCoO_3$ and $SrCoO_{3-\delta}$ powders. In all figures, the spectra have been shifted vertically for clarity.

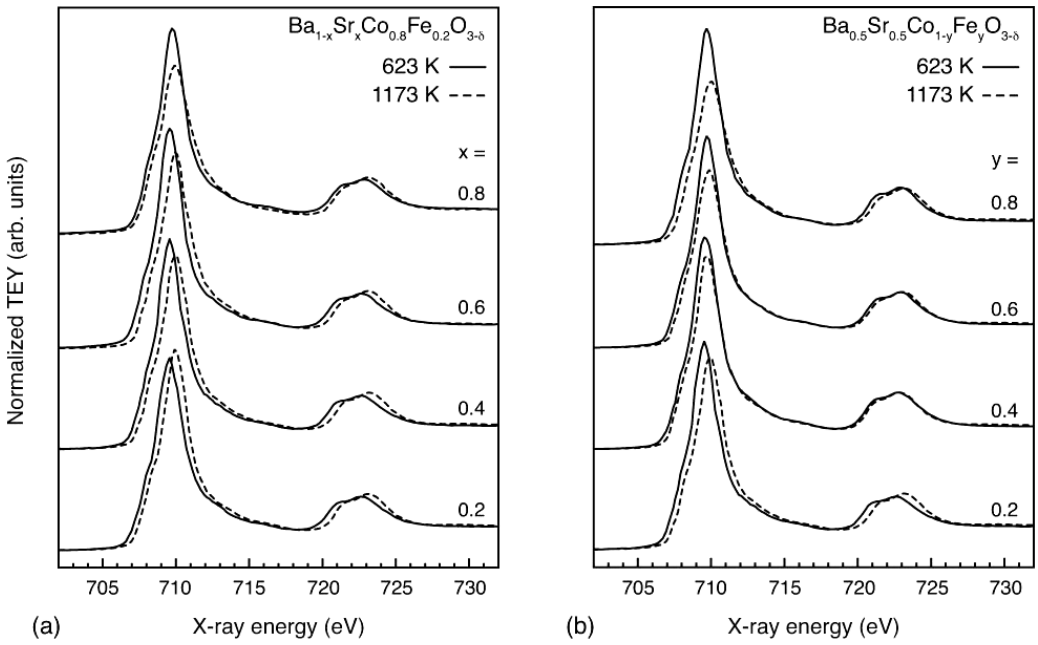

Figure 2. Fe $L_{II,III}$ XAS of (a) $Ba_{1-x}Sr_xCo_{0.8}Fe_{0.2}O_{3-\delta}$ quenched from 623 (solid lines) and 1173 K (dashed lines), and (b) $Ba_{0.5}Sr_{0.5}Co_{1-y}Fe_yO_{3-\delta}$ quenched from 623 and 1173 K. This shows that increasing the quenching temperature most strongly affects Fe in the samples with the highest Sr and Fe content, as evidenced by the reduction in the L_{III} peak intensity relative to that of the L_{II}.

in figure 3(a), while figure 3(b) shows results from varying Co/Fe and temperature. Note that the strong Ba $M_{IV,V}$ white lines overlap in energy with the Co $L_{II,III}$, and some details of the Co spectra are lost. What can be definitively seen in the spectra is that the ratio of the L_{III} to L_{II} peaks increases with higher quenching temperature, contrary to what was observed for the Fe $L_{II,III}$ spectra, which could indicate the conversion of Co^{4+} to Co^{3+}, a reasonable occurrence at 1173 K. As is expected, with a greater amount of Co in the composition, the Co peaks are stronger and the change in the $L_{II,III}$ peak ratio is more prominent. The chemical shifts of both the Fe and Co spectra are negligible with changing composition and quenching temperature.

The transition metal $L_{II,III}$ spectra are useful in determining the spin state of the ions as well as the 3d occupancy and site symmetry of Fe and Co. The branching ratio, mathematically the fractional probability for transitions from the L_{III} level, has been shown to increase from d^0 to

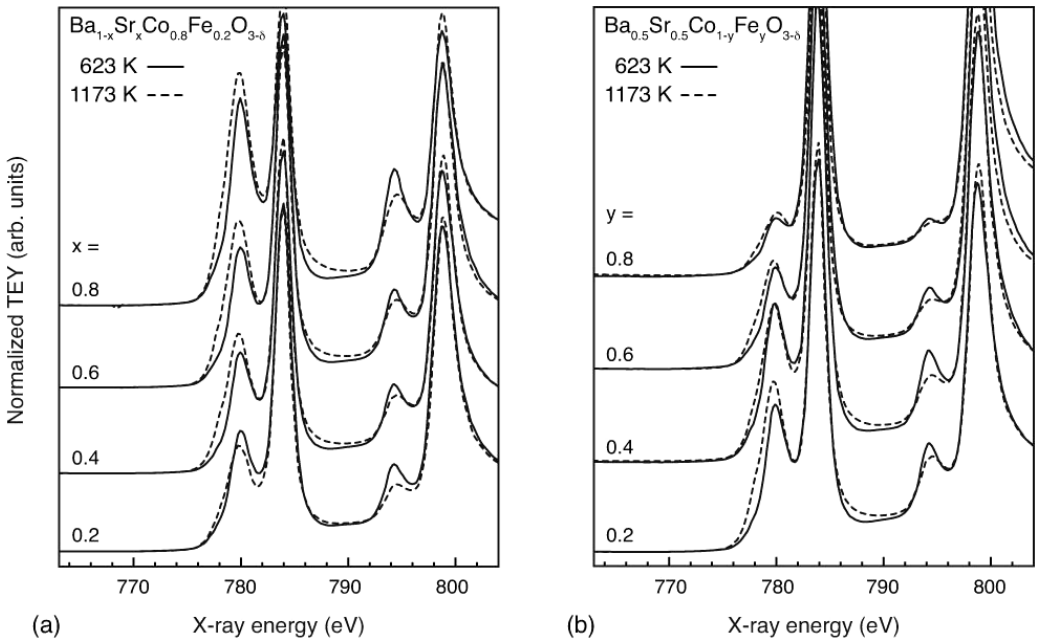

Figure 3. Co $L_{II,III}$ and Ba $M_{IV,V}$ XAS of (a) $Ba_{1-x}Sr_xCo_{0.8}Fe_{0.2}O_{3-\delta}$ quenched from 623 (solid lines) and 1173 K (dashed lines), and (b) $Ba_{0.5}Sr_{0.5}Co_{1-y}Fe_yO_{3-\delta}$ quenched from 623 and 1173 K.

d^5 and then decrease somewhat from d^5 to d^9 for high spin cations [38–40]. Low spin cations have smaller branching ratios than their high spin counterparts. A change in the branching ratio is observed in both the Fe and Co spectra with higher temperature quenching, however, there are no significant chemical shifts evident in the data, which necessarily occur with a change in oxidation state [32, 41].

Since little change in average oxidation state occurs with varying the quenching temperature or chemical composition, the changes in the $L_{II,III}$ XAS are related to the lowering of symmetry that occurs with an increase in oxygen non-stoichiometry, the effect of ligand holes $\underline{L}$, a change in the covalency of the ground state, or a spin transition [26]. For Fe, the small changes in the branching ratio could reflect a reduction of a small amount of Fe^{4+} to Fe^{3+}. The Co branching ratio change is more dramatic: the values for samples quenched from 623 K are very close to those for $LaCoO_3$ and $SrCoO_{3-\delta}$, materials that have mixed or intermediate Co spin states at room temperature. With the increase in branching ratio upon quenching from 1173 K, it seems that in BSCF, Co undergoes a transition from mixed/intermediate to high spin from 623 to 1173 K. The slight increase in intensity at approximately 778 eV in the Co spectra of the 1173 K quenched samples—a minor shoulder on the L_{III} peak—could additionally show that a higher spin state was successfully quenched in [32]. Spectra at the O K edge, discussed below, add more information about the electronic structure and show why only minor changes are present in the transition metal spectra.

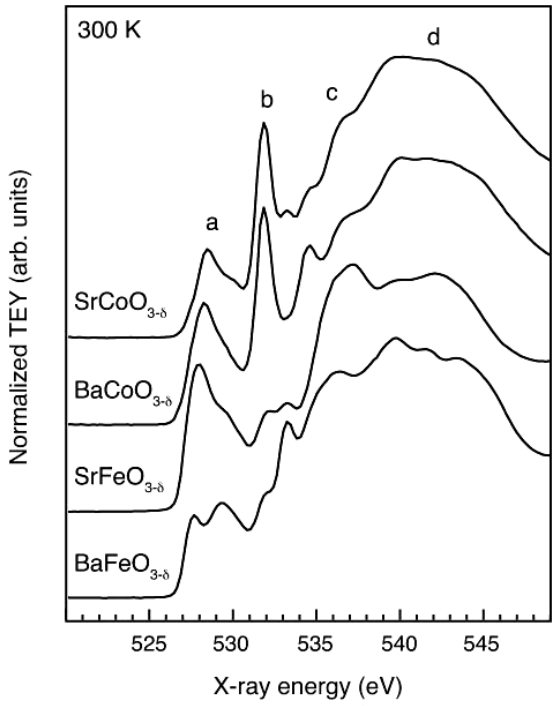

Figure 4. O K XAS of $SrFeO_{3-\delta}$, $SrCoO_{3-\delta}$, $BaFeO_{3-\delta}$, and $BaCoO_{3-\delta}$ powders calcined, slowly cooled, and measured at 300 K. The peaks labeled (a) in the spectra result from the hybridization of the O 2p with the transition metal 3d levels split by the ligand field, peak (b) is ascribed to the development of a carbonate or presence of an adsorbed species, regions (c) and (d) are contributions from the Ba 5d, Sr 4d, and Co/Fe 4sp levels.

3.3. O K XAS

Spectra of $SrFeO_{3-\delta}$ and $SrCoO_{3-\delta}$ as well as $BaFeO_{3-\delta}$ and $BaCoO_{3-\delta}$ are shown in figure 4. The peaks labeled (a) result from transitions from the O 1s level to the O 2p mixed with the transition metal 3d. Higher energy peaks (c) and (d) reflect the Sr 4d, Ba 5d, and Fe/Co 4 sp unoccupied states, respectively, while peak (b) is possibly the result of a contaminating species

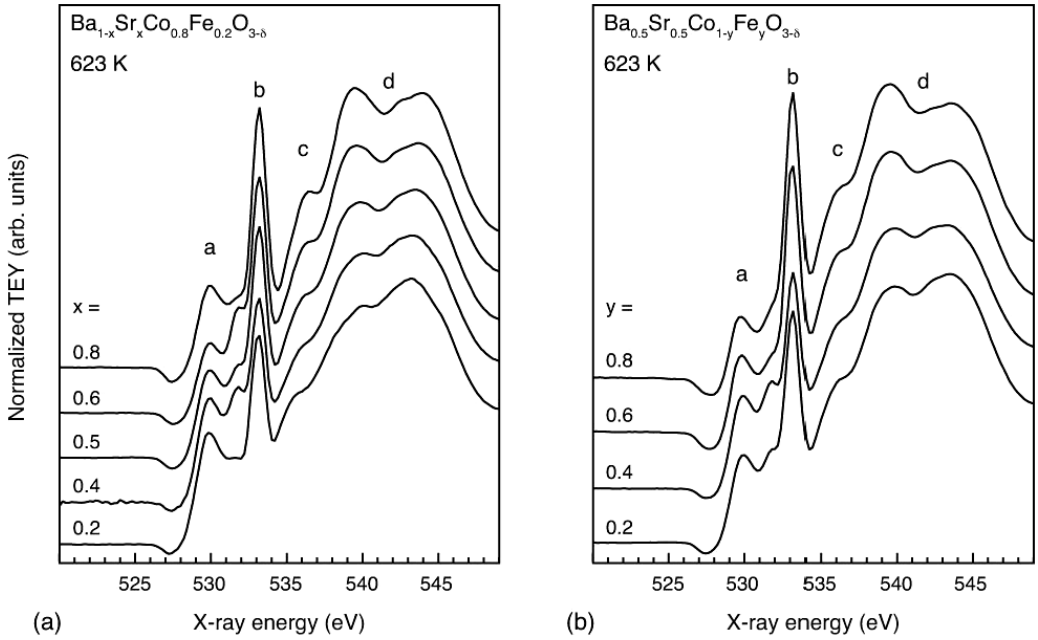

Figure 5. O K XAS of (a) $Ba_{1-x}Sr_xCo_{0.8}Fe_{0.2}O_{3-\delta}$ and (b) $Ba_{0.5}Sr_{0.5}Co_{1-y}Fe_yO_{3-\delta}$ quenched from 623 K. Region (a) is actually comprised of two peaks, showing the ligand field splitting of the transition metal 3d level and the unoccupied e_g and t_{2g} states.

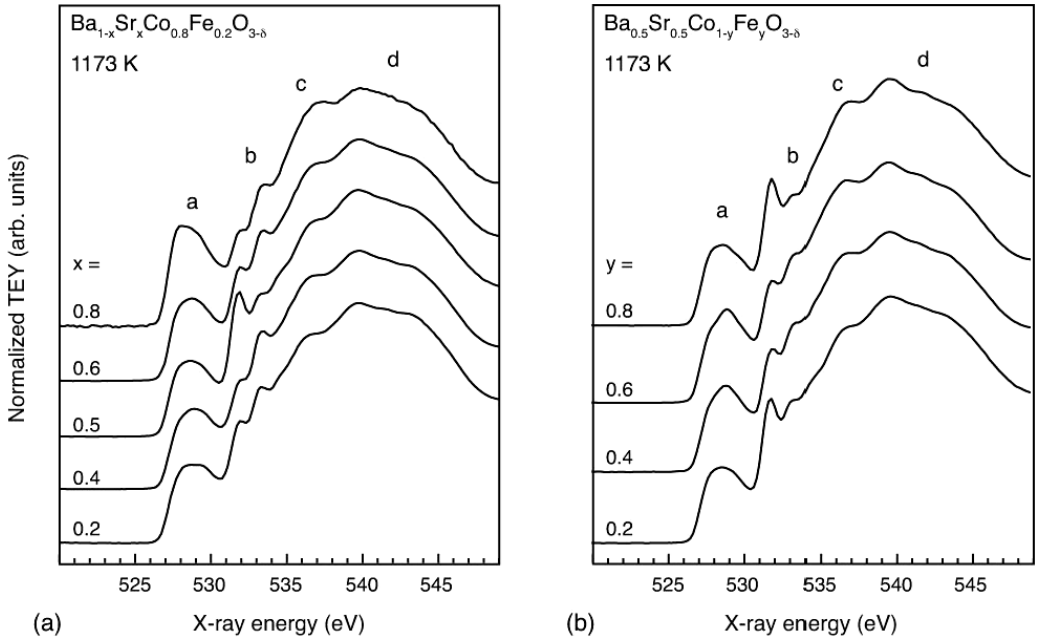

Figure 6. O K XAS of (a) $Ba_{1-x}Sr_xCo_{0.8}Fe_{0.2}O_{3-\delta}$ and (b) $Ba_{0.5}Sr_{0.5}Co_{1-y}Fe_yO_{3-\delta}$ quenched from 1173 K. An intense shoulder on the low energy side of peak (a) has developed indicating the formation of new unoccupied states. The carbonate species is incorporated into the perovskite structure at high temperature, and so peak (b) is reflective of the Sr 4d contribution.

as described below. Figure 5 shows the O K spectra from BSCF samples quenched from 623 K. The results from modifying the Ba/Sr ratio and Co/Fe ratio are shown in figures 5(a) and (b), respectively. Figure 6 shows similar data resulting from BSCF samples quenched from 1173 K. It is in these spectra that large changes are observed between samples quenched at different temperatures and lesser but non-trivial changes are seen with varying composition.

Regions of the BSCF spectra are labeled from lowest to highest energy as (a), (b), (c), and (d). Peak (b) is sharp and more pronounced in the samples that were quenched from 623 K than those from 1173 K; this feature is most likely the result of carbon-based impurities developed in the material or adsorbed on the surface [42, 43]. Unfortunately, the effects of surface contaminants are non-negligible in the TEY mode of XAS collection, with a probing depth maximum

Table 2. Fitting results for peaks (a) and (b) in the oxygen K spectra. Peak (a1) represents new unoccupied states, peaks (a2) and (a3) are from the t_{2g} and e_g levels, respectively, and peak (b) shows the carbonate species.

			Peak position (eV)/normalized area			
x	y	T (K)	(a1)	(a2)	(a3)	(b)
0.8	0.2	623		529.8/0.61	531.5/0.85	533.2/1.70
		1173	527.7/0.55	529.1/1.13	531.9/0.49	533.3/0.37
0.5	0.2	623		529.8/0.80	531.6/0.91	533.2/1.57
		1173	527.8/0.32	529.1/0.80	531.8/0.77	533.2/0.48
0.2	0.2	623		529.8/1.14	531.5/0.77	533.1/1.40
		1173	527.9/0.23	529.3/1.41	531.9/0.74	533.2/0.46
0.5	0.8	623		529.8/0.48	531.6/0.61	533.2/1.89
		1173	527.8/0.40	529.3/0.89	531.9/0.73	533.1/0.39

Table 3. Conductivity results for selected $Ba_{1-x}Sr_xCo_{1-y}Fe_yO_{3-\delta}$ samples, measured on sintered bars with the four-point method. Transition temperatures are listed as approximations because the onset of metallic conductivity is not abrupt. For $x = 0.8$, $y = 0.2$ the maximum conductivity is significantly higher while the activation energy is significantly lower than the other samples. The transition temperature of BSCF with $x = 0.2$, $y = 0.2$ is about 200 K higher than the others due to a possible phase change that only this sample undergoes.

x	y	Maximum total conductivity (S cm^{-1})	Semiconductor activation energy (eV)	Semiconductor–metal transition temperature (K)
0.8	0.2	253.9	0.15	723
0.5	0.2	57.77	0.34	763
0.2	0.2	44.43	0.21	943
0.5	0.8	45.98	0.25	783

of 5–10 nm. If peak (b) results from a crystalline carbonate formation instead of a molecular species, it is possible that additional fine structure is superimposed on the BSCF XAS. To rule out the possibility of surface contamination, a single crystal scraped *in situ* could be used. In the electron energy-loss spectra (EELS) of $SrCoO_3$, where the technique has much higher spatial resolution than x-ray methods, the O K edge has first a sharp peak followed by a second, broader peak about 6 eV higher in energy [44]. In the case of the XAS shown here, this would affect the (d) region, overlapping with contributions from the Fe/Co 4sp orbitals, which are not of particular interest in our case. So far, only one study on the EELS of BSCF with $x = 0.5$, $y = 0.2$ and no XAS on any composition has been performed. The oxygen K edge results presented here are broadly similar to those found with EELS [45], but it should be noted that the energy resolution is significantly better for XAS than for EELS. Additionally, in the spectra of samples quenched from 623 K, a small negative dip is present before the edge onset, which could signal sample charging as might be expected with the semiconducting material.

A main utility of the O K edge for metal oxides lies in the fact that it represents transitions to the O 2p unoccupied states, which are hybridized with those of the metallic species. So, in effect, the O K spectra show the unoccupied p-projected density of states (DOS) of the cations. Considering that metallic electron/hole conduction in perovskite oxides is attributed to the position and occupancy of the transition metal 3d states, the spectral region nearest the Fermi energy that shows the 3d contribution to the O K spectra is most interesting. In the present experimental spectra, this is labeled as (a) in figures 5 and 6, at approximately 527–532 eV. Here, the result of the octahedral crystal field splitting of the 3d level into t_{2g} and e_g symmetries at about 530 and 532 eV, respectively, is evident. This double-peak fine structure is evidence of the cations' high spin states, with $\Delta_{ex} > 10Dq$. The values of the crystal field splitting and transition metal 3d bandwidth are estimated from these peaks to be $10Dq = 1.6$–1.8 eV and $W = 1.1$–1.4 eV in samples quenched from 623 K; there is a slight upward trend in the bandwidth with increasing Co content. The O K edge was fitted with an arctangent step-like function and several Gaussian peaks, the results of which are shown in table 2. Region (a) was given particular focus, with the use of two Gaussians to fit the t_{2g} and e_g components and a third to fit the newly created unoccupied states at 1173 K.

In comparing the results of different quenching temperatures, the most obvious difference in region (a) is the development of a peak just below 528 eV in the 1173 K samples that is not present at 623 K. Also, the crystal field splitting increases by about 1 eV at 1173 K as compared to 623 K. For the samples with $y = 0.2$, a transfer of spectral weight from the e_g to the t_{2g} band is shown by the fitting. The first observation especially indicates that with the higher quenching temperature, new unoccupied states just above the Fermi level (E_F) are created, which links nicely to the appearance of metallic conductivity via hole formation. The sample with the greatest amount of added spectral weight near E_F is $x = 0.8$, $y = 0.2$, which is also the sample with the highest total conductivity as shown in table 3. Other changes in the spectra with higher temperature quenching are the disappearance of the carbonate-based peak at (b) and the smearing out of the higher energy features from 535 eV onward.

4. Discussion

Spectroscopically, the effect of heating the BSCF samples to 1173 K is similar to what happens when a stoichiometric,

charge-neutral material like $La^{3+}Fe^{3+}O_3$ or $La^{3+}Co^{3+}O_3$ is hole-doped by the addition of Sr^{2+} [26, 46, 47]. In the case of BSCF, it has been shown that the perovskite structure is stable with high levels of oxygen deficiency, and the treatment and quenching of samples up to 1173 K for 24 h induced oxygen loss preserved by air quenching to room temperature. The coincidence of the minor changes in the transition metal $L_{II,III}$ spectra with the major changes in the O K spectra upon quenching from high temperature, particularly in the region associated with O–B hybridization, leads us to deduce that oxygen loss with higher temperatures does not create a significant change in the transition metal oxidation state, but instead creates new unoccupied states with a majority O 2p character.

Based on structural data and theory, it has been discussed that the ability of the BSCF system to form stable cubic perovskites alone is evidence that the cations are present in the 3+ oxidation state [22]. The Goldschmidt tolerance factor t is defined by the ionic radii of the perovskite (ABO_3) components: $t = (r_A + r_O)/(\sqrt{2}r_B + r_O)$ [48]. Until the investigation of BSCF, it was accepted that the perovskite structure could only be achieved if t were between 0.75 and 1.0 [49]. To maintain electroneutrality in the material where both Ba and Sr have the 2+ oxidation state, it would be expected that Co and Fe take on at least some degree of the 4+ oxidation state. However, calculating the tolerance factor with 4+ cations yields values greater than 1.0. Taken in conjunction with findings that BSCF has inherently high oxygen deficiency [21], it seems that the preferred thermodynamic oxidation state of the B-site cations is 3+, which lowers the tolerance factor to values more reasonable for the formation of the cubic perovskite. While Mössbauer spectra of the Sr-free and Co-rich composition $BaCo_{0.8}Fe_{0.2}O_{3-\delta}$ did confirm that little Fe^{4+} was present in both a sample annealed at 973 K and one quenched from 1073 K in liquid N_2, it was estimated that all of the Co was 4+ in the annealed sample, likewise almost half in the quenched [50]. The XAS data presented here confirm that the ground state of Fe is high spin $3d^5\underline{L}$, but the state of the Co cations, while probably intermediate spin $3d^6\underline{L}$, is still not fully determined. Notably, while the tolerance factor calculation advances the ideas of high oxygen deficiency and lower cation oxidation states in order to form the cubic perovskite, typically in these kinds of materials a high degree of oxygen deficiency leads to vacancy ordering and structural transformations, from cubic through tetragonal to orthorhombic symmetry with increasing oxygen deficiency, as in $SrFeO_{3-\delta}$ and $SrCoO_{3-\delta}$ [51, 52]. While this structural change is expected for values of $\delta \geqslant 0.5$, McIntosh *et al* have shown that it does not occur in BSCF [11]. That BSCF maintains disorder regardless of temperature or composition has important implications as discussed below.

At temperatures where BSCF is a semiconductor, the site-to-site hopping of thermally activated holes is facilitated by the variation in valence states between the Fe and Co ions. In other perovskites that show conductivity behavior similar to BSCF, a common compositional modification is to start with $A^{3+}B^{3+}O_3$ and substitute at the A-site an ion with a 2+ oxidation state. This has the theoretical effect of introducing electron holes by changing the B-site transition metal valence, but it has been shown that the holes also take on a degree of O 2p character [26]. When the A^{2+} ion is no longer a dopant, but instead forms the parent compound, as in $A^{2+}BO_3$, the ground state is often best described with most of the charge balanced by ligand holes [6, 8]. It is not obvious what effect doping a different A^{2+} ion at the A^{2+} site would have on the electronic structure. In the case of BSCF, Ba^{2+} has a larger radius than Sr^{2+}, so it is likely that the slight structural modifications that accompany an increase in Ba content adjust the way in which the B and O ions interact. This mainly shows up in the B–O–B bond angles and the attractive/repulsive forces between B 3d and O 2p electrons. Increasing the deviation of the B–O–B bond angle from 180°, i.e. tilting neighboring BO_6 octahedra, decreases the degree of hybridization between B 3d and O 2p orbitals, but decreasing the B–O–B bond length increases the hybridization, so a competition of forces is present. In conjunction with the increased hybridization comes an increase in the 3d bandwidths.

Since Co and Fe are much more similar in size than Ba and Sr, and are shown to be in an average 3+ state across the compositions and temperatures here, it is not surprising that the conductivity is influenced more by varying the Ba/Sr ratio than the Co/Fe (see table 3, to be elaborated upon in a future publication) [23]. Previous reports have shown that the maximum total conductivity in BSCF increases with increasing concentration of Co and Sr [13, 14] in agreement with our finding that the 3d bandwidth tracks with Co content and past work showing that the mobility of p-type carriers in $LaFeO_3$ is three orders of magnitude smaller than in $LaCoO_3$ [53]. This conductivity behavior in the cubic perovskite BSCF samples, a monotonic increase with Co content [13], is similar to the Ruddlesden–Popper materials $Sr_3Co_{2-y}Fe_yO_7$, which is linked to a decrease in the transfer integral from Fe to Co [54]. In the samples examined in this study, BSCF with $x = 0.8$ and $y = 0.2$ had by far the highest total conductivity at a value of 253.9 S cm^{-1}, and this composition also showed the greatest increase in unoccupied states near E_F, which points to these holes as the route of metallic conduction. For all samples but $x = 0.2$, $y = 0.2$, the onset of metallic conductivity occurs gradually with increasing temperature as the structure expands, B–O–B bond angles reach the ideal 180°, and the thermal creation of holes that occurs in the semiconducting temperature range becomes saturated.

Both $SrFeO_{3-\delta}$ and $SrCoO_{3-\delta}$ are metallic conductors down to temperatures of 4 K and have been identified as negative charge-transfer materials, with the former antiferromagnetic and the latter ferromagnetic [5, 6, 8]. That most BSCF compositions are in the cubic perovskite structure with B–O–B angles close to or at 180° and the material is not metallic at room temperature puts into question whether BSCF behaves like two of its parent compounds and has negative charge-transfer energy as for the $SrCo_{1-y}Fe_yO_{3-\delta}$ system. If BSCF were a negative charge-transfer material, a p–p energy gap would have to exist to explain the semiconductor behavior, with fluctuations of the type $d^{n+1}\underline{L} + d^{n+1}\underline{L} \rightarrow d^{n+1} + d^{n+1}\underline{L}^2$. It was shown that in the perovskite structure such a gap is not

feasible [55], but if we here consider the effects of a stochastic mixture of Ba/Sr at the perovskite A site, Co/Fe at the B site, and O/vacancy at the O site, Anderson localization [56, 57] comes into play and a negative charge-transfer energy could be suppressed. With increasing temperature, a transition to metallic conductivity with the negative charge-transfer energy dominant occurs as the charge carriers gain enough energy to overcome the differences in neighboring potential wells. In addition to disorder effects, the strength of hybridization between Co/Fe and O contributes to the presence of a p–p gap [54, 55].

5. Summary

$Ba_{1-x}Sr_xCo_{0.8}Fe_{0.2}O_{3-\delta}$ ($x = 0.2, 0.4, 0.5, 0.6, 0.8$) and $Ba_{0.5}Sr_{0.5}Co_{1-y}Fe_yO_{3-\delta}$ ($y = 0.2, 0.4, 0.6, 0.8$) powders quenched from 623 and 1173 K in air were studied with XAS. The $L_{II,III}$ transition metal spectra show that at both quenching temperatures and regardless of composition, the ground state of Fe (Co) is $3d^5\underline{L}$ ($3d^6\underline{L}$). To state a quantitative value for the percentage of each state for each ion requires cluster interaction or multiplet calculations. The oxygen K spectra show that Fe and Co are in their respective high spin states when quenched from high temperatures and that additional hole states with majority O 2p character are created in the metallic temperature. These states are the pathway through which holes are metallically conducted via the B–O–B bonding. To better understand the conductivity, measurement of the Seebeck coefficient for BSCF would help by quantifying the carrier concentration. Based on the apparently high amount of ligand holes in the ground state of BSCF, it is proposed that this material has a negative charge-transfer energy and that semiconductivity is induced by Anderson localization.

Acknowledgments

The synchrotron work was performed on beamline 1.1 of the Daresbury Laboratory Synchrotron Radiation Source (SRS). Funding for the project was granted by the UK Science and Technology Facilities Council under SRS project No. 47093.

References

[1] Cava R J, Batlogg B, Krajewski J J, Farrow R, Rupp L W, White A E, Short K, Peck W F and Kometani T 1988 *Nature* **332** 814
[2] von Helmolt R, Wecker J, Holzapfel B, Schultz L and Samwer K 1993 *Phys. Rev. Lett.* **71** 2331
[3] Coey J M D, Viret M and von Molnar S 1999 *Adv. Phys.* **48** 167
[4] Korotin M A, Ezhov S Y, Solovyev I V, Anisimov V I, Khomskii D I and Sawatzky G A 1996 *Phys. Rev.* B **54** 5309
[5] Abbate M, Zampieri G, Okamoto J, Fujimori A, Kawasaki S and Takano M 2002 *Phys. Rev.* B **65** 165120
[6] Bocquet A E, Fujimori A, Mizokawa T, Saitoh T, Namatame H, Suga S, Kimizuka N, Takeda Y and Takano M 1992 *Phys. Rev.* B **45** 1561
[7] Bocquet A E, Mizokawa T, Saitoh T, Namatame H and Fujimori A 1992 *Phys. Rev.* B **46** 3771
[8] Potze R H, Sawatzky G A and Abbate M 1995 *Phys. Rev.* B **51** 11501
[9] Zaanen J, Sawatzky G A and Allen J W 1985 *Phys. Rev. Lett.* **55** 418
[10] Kamata K, Nakamura T and Sata T 1974 *Bull. Tokyo Inst. Technol.* **120** 73
[11] McIntosh S, Vente J F, Haije W G, Blank D H A and Bouwmeester H J M 2006 *Chem. Mater.* **18** 2187
[12] Shao Z P, Yang W S, Cong Y, Dong H, Tong J H and Xiong G X 2000 *J. Membr. Sci.* **172** 177
[13] Chen Z H, Ran R, Zhou W, Shao Z P and Liu S M 2007 *Electrochim. Acta* **52** 7343
[14] Wei B, Lu Z, Huang X Q, Miao J P, Sha X Q, Xin X S and Su W H 2006 *J. Eur. Ceram. Soc.* **26** 2827
[15] Anderson P W 1950 *Phys. Rev.* **79** 350
[16] Zener C 1951 *Phys. Rev.* **82** 403
[17] Shao Z P and Haile S M 2004 *Nature* **431** 170
[18] Yan A, Cheng M, Dong Y L, Yang W S, Maragou V, Song S Q and Tsiakaras P 2006 *Appl. Catal.* B **66** 64
[19] Lebon A, Adler P, Bernhard C, Boris A V, Pimenov A V, Maljuk A, Lin C T, Ulrich C and Keimer B 2004 *Phys. Rev. Lett.* **92** 037202
[20] Taguchi H, Shimada M and Koizumi M 1980 *Mater. Res. Bull.* **15** 165
[21] McIntosh S, Vente J F, Haije W G, Blank D H A and Bouwmeester H J M 2006 *Solid State Ion.* **177** 1737
[22] Shao Z P, Xiong G X, Tong J H, Dong H and Yang W S 2001 *Sep. Purif. Technol.* **25** 419
[23] Yang Z, Harvey A S, Infortuna A and Gauckler L J 2008 *J. Appl. Crystallogr.* submitted
[24] Teraoka Y, Yoshimatsu M, Yamazoe N and Seiyama T 1984 *Chem. Lett.* **13** 893
[25] Singh S K and Kumar J 2006 *J. Phys. Chem. Solids* **67** 1687
[26] Abbate M *et al* 1992 *Phys. Rev.* B **46** 4511
[27] Surman M *et al* 1992 *Rev. Sci. Instrum.* **63** 4349
[28] Crocombette J P, Pollak M, Jollet F, Thromat N and Gautier-Soyer M 1995 *Phys. Rev.* B **52** 3143
[29] Newville M 2001 *J. Synchrotron Radiat.* **8** 322
[30] Wang H H, Tablet C, Feldhoff A and Caro H 2005 *J. Membr. Sci.* **262** 20
[31] Shannon R D 1976 *Acta Crystallogr.* A **32** 751
[32] Abbate M, Fuggle J C, Fujimori A, Tjeng L H, Chen C T, Potze R, Sawatzky G A, Eisaki H and Uchida S 1993 *Phys. Rev.* B **47** 16124
[33] Hu Z *et al* 2002 *J. Alloys Compounds* **343** 5
[34] Kuepper K, Balasz I, Hesse H, Winiarski A, Prince K C, Matteucci M, Wett D, Szargan R, Burzo E and Neumann M 2004 *Phys. Status Solidi* a **201** 3252
[35] Okamoto J *et al* 2005 *Phys. Rev.* B **71** 104401
[36] Chainani A, Mathew M and Sarma D D 1993 *Phys. Rev.* B **48** 14818
[37] Grenier J, Ea N, Pouchard M and Abou-Sekkina M M 1984 *Mater. Res. Bull.* **19** 1301
[38] Graetz J, Ahn C C, Ouyang H, Rez P and Fultz B 2004 *Phys. Rev.* B **69** 235103
[39] Pearson D H, Ahn C C and Fultz B 1993 *Phys. Rev.* B **47** 8471
[40] Thole B T and van der Laan G 1988 *Phys. Rev.* B **38** 3158
[41] Tafto J and Krivanek O L 1982 *Phys. Rev. Lett.* **48** 560
[42] Butorin S M *et al* 1994 *J. Phys.: Condens. Matter* **6** 9267
[43] Haas O, Ludwig C and Wokaun A 2006 *Anal. Chem.* **78** 7273
[44] Mansot J L, Golabkan V, Romana L and Césaire T 2003 *J. Microsc.* **210** 110
[45] Arnold M, Wang H H and Feldhoff A 2007 *J. Membr. Sci.* **293** 44
[46] Moodenbaugh A R, Nielsen B, Sambasivan S, Fischer D A, Friessnegg T, Aggarwal S, Ramesh R and Pfeffer R L 2000 *Phys. Rev.* B **61** 5666
[47] Wadati H *et al* 2005 *Phys. Rev.* B **71** 035108
[48] Goldschmidt V M 1926 *Naturwissenschaften* **14** 477
[49] Ramadass N 1978 *Mater. Sci. Eng.* **36** 231

[50] Nomura K, Goda T, Ujihira Y, Hayakawa T and Takehira K 1991 *Hyperfine Interact.* **69** 835
[51] Takeda Y, Kanno R, Takada T, Yamamoto O, Takano M, Nakayama N and Bando Y 1986 *J. Solid State Chem.* **63** 237
[52] Takeda Y, Kanno R, Takada T, Yamamoto O, Takano M and Bando Y 1986 *Z. Anorg. Allg. Chem.* **541** 259
[53] Gaur K, Verma S C and Lal H B 1988 *J. Mater. Sci.* **23** 1725
[54] Abbate M, Mogni L, Prado F and Caneiro A 2005 *Phys. Rev.* B **71** 195113
[55] Mizokawa T, Namatame H, Fujimori A, Akeyama K, Kondoh H, Kuroda H and Kosugi N 1991 *Phys. Rev. Lett.* **67** 1638
[56] Anderson P W 1958 *Phys. Rev.* **109** 1492
[57] Mott N 1968 *Rev. Mod. Phys.* **40** 677